URSI AP-RASC, Sydney, Australia, 17 – 22 August 2025

Radio Channel Measurements at mmWave Band for Body-to-Vehicle Networks

Sławomir J. Ambroziak(1), Agnieszka Czapiewska(1), Krzysztof K. Cwalina(1), Piotr Rajchowski(1), Filipe D. Cardoso(2), Manuel M. Ferreira(2), Mariella Särestöniemi(3), Anna Pietrenko-Dąbrowska(1), Sławomir Kozieł(1)(4), and Luis M. Correia(5)
(1) Faculty of Electronics, Telecommunications and Informatics, Gdańsk University of Technology, Gdańsk, Poland
(2) Instituto Politécnico de Setúbal, Escola Superior de Tecnologia de Setúbal, INESC-INOV, 2914-508 Setúbal, Portugal
(3) Centre for Wireless Communications, Faculty of Information Technology and Electrical Engineering & Health Sciences and Technology, Faculty of Medicine, University of Oulu, Oulu, Finland
(4) Engineering Optimization and Modeling Center, Reykjavik University, Reykjavik, Iceland
(5) IST/INESC-INOV, University of Lisbon, 1049-001 Lisbon, Portugal

Abstract

This paper presents measurements of the radio channel at the millimeter-wave band at 28 GHz with a bandwidth of 500 MHz for body-to-vehicle networks. The measurement stand, environment and scenarios are described. The analysis of the preliminary results of the power delay profile is presented. It has been initially shown, that the orientation of the antennas has the greatest impact on the characteristics of the radio channel, while the presence of passengers has has no significant effect.

1 Introduction

Communications between in-vehicle infrastructure and Body Area Network (BAN), operating on the driver's or passenger's body and monitoring various vital signs, fits into one of the 5G use cases, namely vehicle-to-everything (V2X) [1]. This type of off-body communications may also be referred to as body-to-vehicle (B2V). A millimeter-wave (mmWave) communications is considered in 5G New Radio (NR), covering 24.25-52.6 GHz in frequency range FR2 [2]. To design a reliable B2V network, it is important to have a deep knowledge about the radio channel characteristics, e.g., the system loss, the number of multipath components (MPCs), the mean delay and the root mean square (rms) delay spread. This allows the overall communications performance to be optimized [3].

This paper addresses the situation, in which a user (static or dynamic) wearing a mmWave BAN device is in an in-vehicle environment, being alone as a driver or with a passenger on the side seat. These scenarios have been empirically investigated in order to characterize the mmWave B2V radio channel.

2 Measurement Stand

Measurements have been performed with the Microwave Network Analyzer (MNA) Keysight N5227B [4], which is a core of the measurement stand presented in Fig. 1. During the performed studies, port 1 and 2 of the MNA acted as transmitters (Tx), while ports 3 and 4 were receivers (Rx). The MNA has been set up for the measurements of the scattering matrix parameters, i.e., S31, S41, S32, and S42, in time domain, which may be considered as a power delay profiles (PDPs) for these channels. For the Rx antenna, one has selected a dual polarized Quad Ridged Horn Antenna QRH40 [5], with 14 dBi gain and a half power beamwidth (HPBW) of 30° at 28 GHz in both E- and H-planes, regardless polarization.

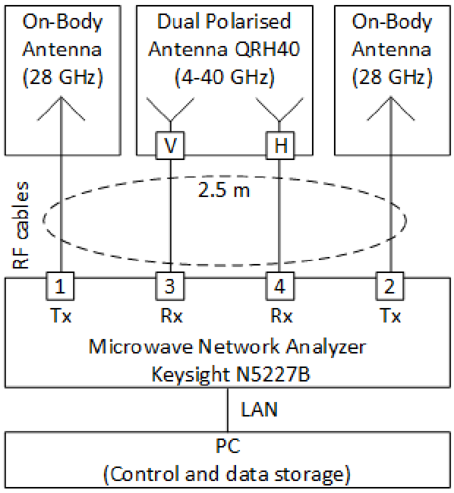

Figure 1. Block diagram of measurement stand.

As the on-body Tx antenna (Fig. 2) a planar monopole antenna, fed by a bottom-grounded coplanar waveguide, was used [6]. It has been designed for wearable applications at 28 GHz, having an impedance bandwidth of 2 GHz, a realized gain around 11 dBi, and a HPBW of ±35°. The reported specific absorption rate (SAR) values are below the IEEE safety standard of 1.6 W/kg [6].

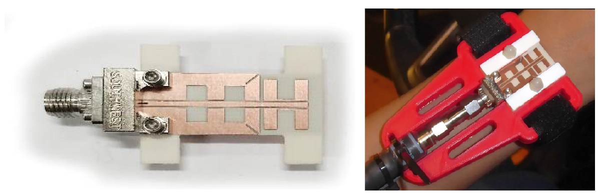

Figure 2. Tx antenna: prototype (left), mounted (right).

All radio frequency (RF) connections were done with MWX061 cables [7]. The MNA was calibrated in order to properly compensate the delays and attenuations in the RF cable tracks. With the calibration step performed, the recorded PDPs correspond to the relative attenuation in between the power at the Tx antenna port and the output power of the Rx antenna ports, i.e., the system loss [8].

The measurement parameters are summarized in Table 1. The test signal was centered at 28 GHz with a bandwidth of 500 MHz, which fits into two FR2 bands: n257 (26.5–29.5 GHz) and n261 (27.5–28.35 GHz). The MNA Tx power was set to 0 dBm. The Intermediate Frequency (IF) filter bandwidth of 100 kHz was used, yielding the average noise level of -88.9 dBm. The Tx pulse duration time was 3.9 ns, and the PDPs were recorded over a 40 ns delay window. In total 4001 sample points are obtained for each PDP. For each scenario 200 PDPs (100 for non-breathing case) measurements have been captured, while the triggering time between successive measurements was varying, being 276 ms in average. The MNA operates in the frequency domain, therefore the Inverse Fourier Transform is performed to obtain the PDP from the measured Transfer Function of the channel. The Kaiser-Bessel window with shape parameter $\beta = 6$ was used in this process.

Table 1. Summary of the measurement parameters.

Tx power	0 dBm
Center frequency	28 GHz
Bandwidth	500 MHz
IF Bandwidth	100 kHz
Tx pulse time	3.9 ns
CIR duration (max. delay)	40 ns
No. of samples per PDP	4001
Window function	Kaiser-Bessel ($\beta = 6$)
Average triggering time	276 ms

The MNA was controlled by a personal computer (PC) via an Ethernet connection. The control software has been designed in graphical programming language (G) used in LabVIEW [9], which allowed for automated measurement process. PC was also responsible for the measurement data storage on a local hard drive; over 5.6 GB of measurement data has been collected.

3 Measurement Environment and Scenarios

As the investigated environment one has selected Ford Grand C-Max, which external dimensions (length, width, height) are $4.520 \times 1.828 \times 1.684$ m. During measurements the car (with closed windows) has been parked in an underground car park of Gdańsk University of Technology and no significant influence of other vehicles or people on the results has been noticed. The MNA has been placed in the middle of the back seat and the PC was placed behind the car while the Ethernet cable was led through the trunk lid.

Scenarios realized during measurements may be categorized and described using an eight-dimensional diagram, as presented in Fig. 3. And so, six placements/orientations of Tx antennas have been considered, named according to the classification proposed in [10]: left and right wrist (AB_L and AB_R), left and right side of the head (HE_L and HE_R), chest with vertical (V) and horizontal (H) polarization (ToFV and ToFH).

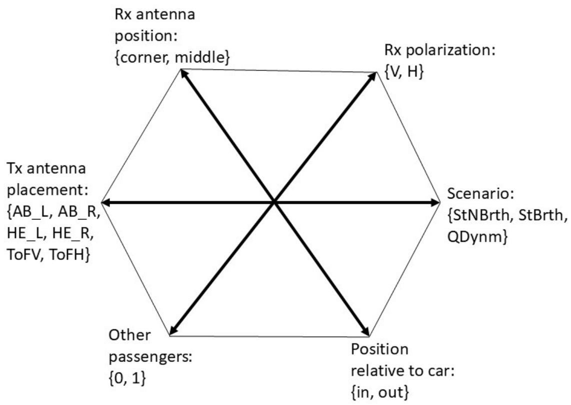

Figure 3. Diagram of realized scenarios.

Regarding Rx antenna, two alternative positions have been considered, namely: middle of the dashboard and upper right corner of the windshield. Additionally, dual-polarized Rx antenna is able to receive both V- and H-polarized electromagnetic waves. In Fig. 4 a mutual orientation of Rx and Tx antennas for exemplary antennas deployment with their HPBW has been presented.

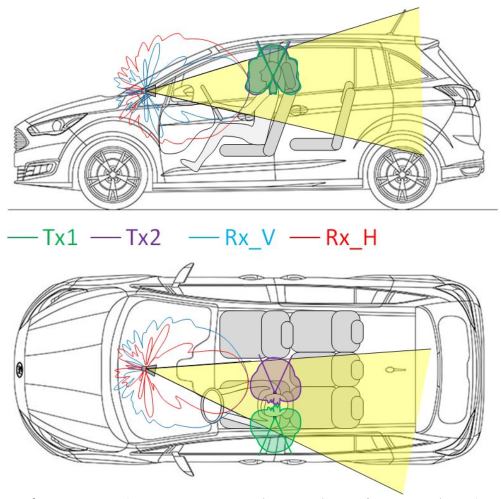

Figure 4. Mutual antennas orientation for Rx in the center of the dashboard and Tx on the head.

Three scenarios of the user behavior have been taken into account: static user normally breathing (StBrth), static user non-breathing (StNBrth), and quasi-dynamic user (QDynm) mimicking car driving. All scenarios have been repeated twice: for only user and for additional person sitting on the side seat as a passenger (see Fig. 5).

The last scenario is related to the user position. In addition

Figure 5. View on the exemplary measurement scenario.

to the user sitting inside the car (in), some measurements have been performed with the user standing outside the car (out), being close to its left door.

4 Preliminary Results

As a preliminary results a few selected PDP graphs have been presented in the following, where gray color is for instantaneous PDP, and black one is for short-term (average) PDP [11]. For the analysis one has selected the scenario with vertically polarized Rx antenna mounted in the middle of the dashboard, on-body Tx antennas mounted on the head of the user sitting inside the car and normally breathing (see Fig. 5). In the graphs one has also presented mean values (μ) and standard deviations (σ) of the time dispersion parameters, namely: the average delay (T_D), number of MPCs (N) and rms delay spread (S), as defined in [11].

In Fig. 6 and Fig. 7 one can analyze the influence of the on-body antenna placement. For the HE_R antenna (Tx2) one can clearly see one MPC, while for the HE_L (Tx1) also a second MPC appears - due to reflections on the car body structure. It results in the higher values of T_D and S. In addition, lower power level may be observed in the second case due to the higher system loss values. It should be noted, that $\mu_{T_D} = 0$ and $\sigma_{T_D} = 0$ mean, that the particular channel is very stable and consists only one MPC, which is the case of static user with HE_R antenna.

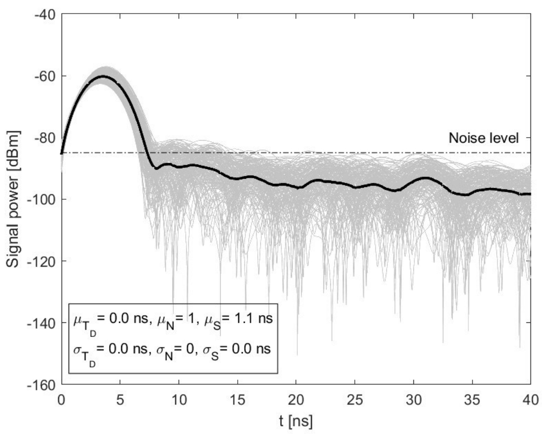

Figure 6. PDP for HE_R, static user and no passenger.

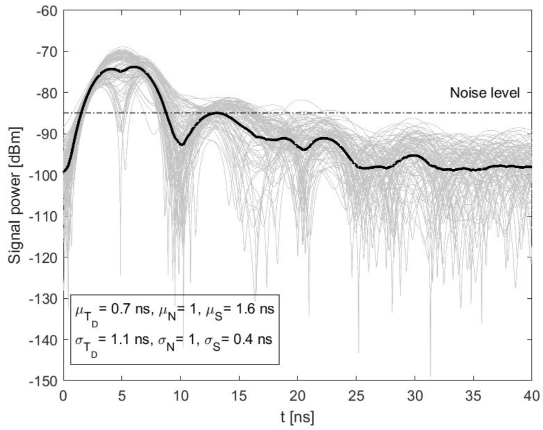

Figure 7. PDP for HE_L, static user and no passenger.

Fig. 8 and Fig. 9 presents the PDPs for scenario with passenger on the side seat, while Fig. 10 and Fig. 11 allow to see the PDPs for the dynamic scenario with user only. By comparing Fig. 6 with Fig. 8 and Fig. 7 with Fig. 9 one can see the influence of the passenger presence: for the HE_R antenna it causes a higher power level of late MPCs due to the signal reflection from the passenger, but for HE_L it is noticeable that the late MPCs have lower power due to the passenger body attenuation. For the former case, time dispersion parameters have similar values, but for the latter these values are noticeably lower.

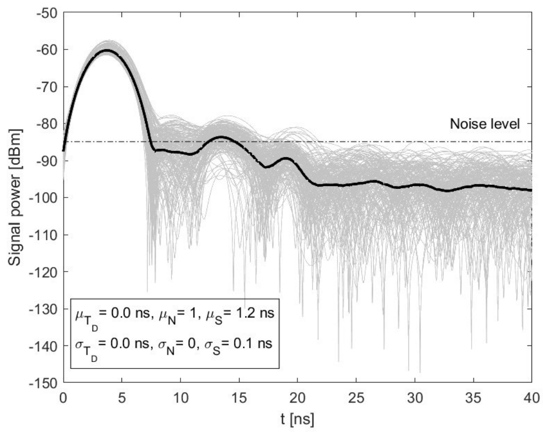

Figure 8. PDP for HE_R, static user and a passenger.

Comparison of Fig. 6 with Fig. 10 and Fig. 7 with Fig. 11 shows that the influence of user dynamics is also different for different location of wearable antennas. For HE_R the user's motion causes higher standard deviation of T_D and S, but for HE_L it results in completely different shape of PDP, lower number od MPCs and lower values of time dispersion parameters.

5 Conclusions

In the paper measurements of the radio channel at the mmWave Band for B2V networks have been presented. The bandwidth of 500 MHz, centered at 28 GHz has been chosen as possible usage frequency for 5G. The measurement stand, including MNA and mmWave antennas, both on-body and external one have been described. The car envi-

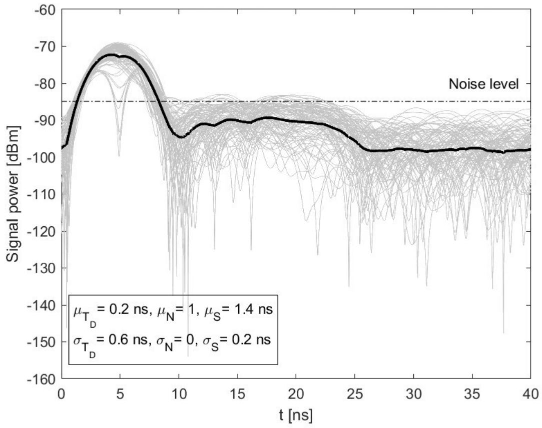

Figure 9. PDP for HE_L, static user and a passenger.

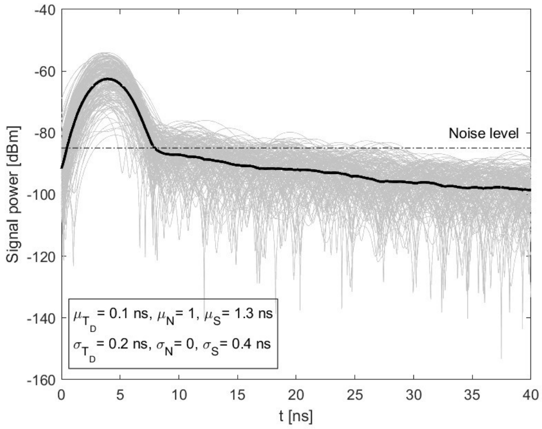

Figure 10. PDP for HE_R, dynamic user and no passenger.

ronment, that has been selected for investigations, has been also presented, as well as the description of all scenarios, that have been realized during investigations.

Analysis of preliminary results focuses on the influence of the on-body antenna placement, presence of the passenger and user dynamics on the statistics of time dispersion parameters, i.e., average delay and rms delay spread. It has been initially shown, that the mutual Tx-Rx antennas orientation has the strongest impact on radio channel characteristics, while the presence of the passenger affects the least. But this aspect, like many others, needs a deeper analysis, that will be done in the future work.

6 Acknowledgements

This publication is based upon work from COST Action INTERACT, CA20120, supported by COST (European Cooperation in Science and Technology). Authors would like to thank Mrs. Hira Manzoor for her contribution to the measurement campaign.

References

[1] A. V. Lopez, et al., "Opportunities and Challenges of mmWave NR," *IEEE Wireless Communications*, **26(2)**, April 2019, pp. 4–6.

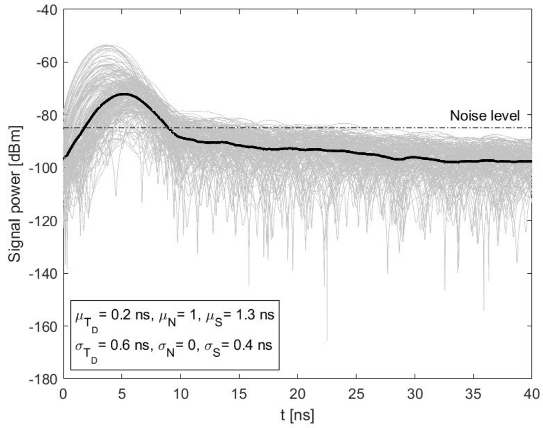

Figure 11. PDP for HE_L, dynamic user and no passenger.

[2] 3GPP TS 38.101-2, "NR; User Equipment (UE) Radio Transmission and Reception; Part 2: Range 2 Standalone," **v. 15.4.0**, Jan. 2019.

[3] S.J. Ambroziak, F.D. Cardoso, M.M. Ferreira, M. Särestöniemi and L.M. Correia, "People's Influence on Indoor Body Area Networks Channel Characteristics," *IEEE Access*, **12**, pp. 184285-184302, Dec. 2024.

[4] Keysight, "Keysight PNA Network Analyzer N5227B 900 Hz to 67 GHz," 2022, [online] Available: https://www.keysight.com/us/en/assets/9018-04327/technical-specifications/9018-04327.pdf.

[5] RF Spin, "Quad Ridged Horn Antenna – Model QRH40," [online] Available: https://www.rfspin.com/product/qrh40/.

[6] U. Ullah, S. Koziel and A. Pietrenko-Dabrowska, "Design and Characterization of a Planar Structure Wideband Millimeter-Wave Antenna With Wide Beamwidth for Wearable Off-Body Communication Applications," *IEEE Antennas and Wireless Propagation Letters*, **21**, 10, Oct. 2022, pp. 2070-2074, doi: 10.1109/LAWP.2022.3190567.

[7] Junkosha, "MWX0 SERIES," [online] Available: https://www.junkosha-mwx.com/products/download/mwx0.pdf.

[8] ITU-R P.341-7, "The Concept of Transmission Loss for Radio Links," Aug. 2019, [online] Available: https://www.itu.int/rec/R-REC-P.341-7-201908-I/en.

[9] https://www.ni.com/pl-pl/shop/labview.html.

[10] M. Mackowiak, "Modelling MIMO Systems in Body Area Networks in Outdoors," *Ph. D. Dissertation*, IST-University of Lisbon, Lisbon, Portugal, 2013.

[11] ITU-R P.1407-8, "Multipath propagation and parameterization of its characteristics," Sep. 2021, [online] Available: https://www.itu.int/dms_pubrec/itu-r/rec/p/R-REC-P.1407-8-202109-I!!PDF-E.pdf.